Observation of separated plasma structure in non-inductive discharge in QUEST

Yuta HIGASHIZONO, Mizuki SAKAMOTO, Yousuke NAKASHIMA[1)], Ryou YONENAGA[1)], Hideki ZUSHI, Kazuaki HANADA, Masaki ISHIGURO, Kazuo NAKAMURA, Hiroshi IDEI, Makoto HASEGAWA, Kohnosuke SATO, Itaru GOUDA[2)], Shoutarou TSURU[2)], Shoji KAWASAKI, Hisatoshi NAKASHIMA, Aki HIGASHIJIMA, Nobuhiro NISHINO[3)], Osamu MITARAI[4)], Takashi MAEKAWA[5)], Yasuaki KISHIMOTO[5)], Yuichi TAKASE[6)] and QUEST Group

Advanced Fusion Research Center, Research Institute for Applied Mechanics, Kyushu University, Kasuga, Fukuoka 816-8580, Japan

[1)] *Plasma Research Center, University of Tsukuba, Tsukuba, Ibaraki 305-8577, Japan*

[2)] *Interdisciplinary Graduate School of Engineering Sciences, Kyushu University, Kasuga, Fukuoka 816-8580, Japan*

[3)] *Department of Mechanical System Engineering, Graduate School of Engineering, Hiroshima, Japan*

[4)] *Kyushu Tokai University, Kumamoto, Japan*

[5)] *Department of Nuclear Engineering, Graduate School of Engineering, Kyoto University, Kyoto, Japan*

[6)] *Graduate School of Frontier Science, The University of Tokyo, Tokyo, Japan*

(Received: 20 November 2009 / Accepted: 23 February 2010)

Non-inductive discharge using an 8.2 GHz electron cyclotron heating wave is performed in QUEST. High-speed (20000 fps) and medium-speed (500 fps) cameras are used to observe the plasma behavior. In an open magnetic field, high-speed camera measurements show that a part of the slab plasma near the center stack separates and moves radially outward. Medium-speed camera measurements show that the separated plasma stops around the second harmonic electron cyclotron region at $R \sim 0.6 - 0.8\ m$. The plasma current, Ip, correspondingly increases during the plasma stagnation and remains higher than at other times during stagnation. After the plasma moves to the outer region near the vacuum chamber, Ip decreases. Hard X-ray measurements in an experiment with the same external magnetic field structure show that the hard X-ray signal increases along with increasing Ip. It suggests that high-energy electrons are generated by the stagnation of the plasma at $R \sim 0.6 - 0.8\ m$.

Keywords: spherical tokamak, non-inductive discharge, H_α image, CCD camera, high energy electron

1. Introduction

Spherical torus (ST) plasma confinement is an efficient method for achieving high beta plasmas. Since an ST has only a limited space at the center stack (CS) region to ensure a low aspect ratio, plasma initiation and ramp-up without an ohmic solenoid is a critical issue. Electron cyclotron heating (ECH) has been used to initiate the plasma and ramp-up the plasma current in many devices [1, 2, 3, 4]. Full non-inductive plasma current; up to 20 kA, in a plasma start-up sequence on a configuration, without a center solenoid was achieved on LATE [3]. Since the physical mechanism of the initiation of plasma current by ECH remains unclear, detailed analysis is needed to clarify the mechanism.

High-speed camera measurements have been used in many magnetic plasma confinement device [5, 6, 7, 8]. Observing the plasma behavior with a high-speed camera is an effective method for visualizing the behavior of edge plasmas as two-dimensional images of visible light emission. The plasma behavior observed by a high-speed camera also provides useful information on the plasma-wall interaction. A monitoring system combining the camera measurement with a software program that can replay captured images just after the plasma discharge, together with the previous 10 images, has been developed. Therefore, the change in H_α emission due to the plasma position and hydrogen recycling in each plasma discharge can be observed.

In the compact spherical tokamak CPD, current ramp up using 8.2 GHz ECH was demonstrated. A CCD camera tangentially viewing a poloidal cross-section of the plasma was applied to CPD. Topological changes in the plasma were observed before and after the current jump. It was reported that the current jump occurs due to slight differences in the operating parameters such as the poloidal field (PF) coil currents, ECH power, and so on [4]. During the current jump, a negative floating potential was observed through directional Langmuir probe measurements. These results suggest that high-energy electrons were

author's e-mail: yuta@triam.kyushu-u.ac.jp

deeply involved with the current start-up. In QUEST, non-inductive discharge using 8.2 GHz begun in 2008. It is crucial to realize the current ramp-up without an ohmic solenoid and clarify in detail the mechanism associated with the current ramp-up.

In this paper, the experimental setup is described in section 2. Experimental results and discussion are presented in section 3. The paper is summarized in section 4.

2. Experimental Setup

Figure 1 shows toroidal (Fig. 1 (a)) and poloidal (Fig. 1 (b)) cross-sections of QUEST, a medium sized spherical tokamak device whose chamber height is 2.8 m and radius is 1.4 m. The diameter of the CS is 0.4 m. The major (R) and minor radii of the plasma are 0.68 m and 0.4 m, respectively. In this paper, the Z-axis and R-axis correspond to the vertical and radial directions, respectively, as shown in the poloidal cross section. Eight toroidal field (TF) coils produce the toroidal magnetic field, $Bt \sim 0.25$ T at $R \sim 0.64$ m. PF coils are used to create the vertical field, Bv. The magnetic field for plasma confinement is optimized by adjusting the TF and PF. The plasma discharge described in this paper is sustained using hydrogen gas puffing and ECH by 8.2 GHz klystrons. The maximum ECH power is 200 kW. In a typical experiment, the plasma discharge is operated at five-minute intervals. In Fig. 1 (b), the external magnetic field described in this paper is shown. Straight lines at $R \sim 0.33$ m and $R \sim 0.66$ m correspond to the first and second harmonic regions of ECH, respectively in the case of a TF current of ~ 30 kA.

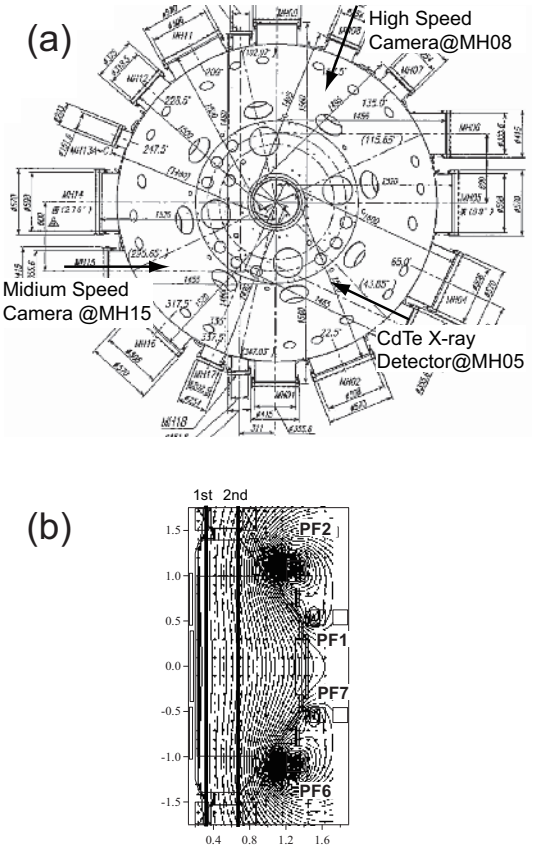

Fig. 1 (a) Top view of QUEST chamber and installation positions of high-speed camera, medium-speed camera and X-ray detector. (b) Poloidal cross-sectional view of QUEST.

A high-speed camera (NAC K5) and a medium-speed camera (DITECT HAS-220) are installed in $MH08$ and $MH15$ ports of QUEST, respectively. Both cameras view the poloidal cross-sections from the horizontal ports. In this paper, the frame speed of the high speed camera and medium-speed camera is 20000 fps and 500 fps. An interference filter that transmits 75% of light at wavelengths from 650 nm to 690 nm is attached in front of a lens so that only H_α-light (656.3 nm) can be observed in the plasma. These cameras are connected to a PC in the QUEST machine room. Two-dimensional images are captured during the QUEST experiment just after the PC in the machine room receives a trigger signal, which is synchronized with the start-up of the coil current.

Hard X-ray measurements were performed using semiconductor detectors (CdTe). The detector measures the range of $3-200$ keV at an efficiency of more than $>$ 0.3. Raw signals are recorded every 0.2 μs to study the quick response of hard X-rays just after the RF waves are injected. Fast electrons collide with ions and bulk electrons and radiate in the hard X-ray range of the spectrum.

3. Experimental Results and Discussion

3.1 Bv dependence of plasma current

A vertical field scan experiment in an open magnetic field structure was performed on non-inductive discharge #3749. In this experiment, gas was puffed at 0.15 s for 0.1 s. After gas injection, the base pressure increased from 2.5×10^{-7} $Torr$ to 1.3×10^{-6} $Torr$.

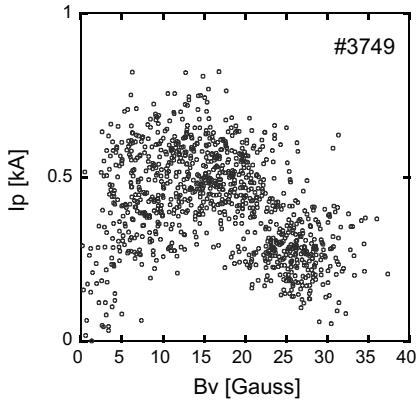

Fig. 2 Bv dependence of Ip in #3749.

Plasma was produced by 8.2 GHz ECH at 0.4 s and terminated at 0.65 s. The RF power and TF current were kept almost constant at 85 kW and 30 kA, respectively for the entire plasma duration. The currents of poloidal coils 1, 7 ($PF1,7$) and 2, 6 ($PF2,6$) were increased at the same rate. Thus, the n-index (decay index) was kept constant during the discharge. Figure 2 shows the Bv dependence of Ip. In this shot, the vertical field increased from 0 to 35 G at $R \sim 0.64$ m and $Z \sim 0.0$ m. As shown in this figure, Ip was maximum at a Bv of $10-15$ G.

3.2 Relationship between plasma current and plasma behavior

At shot number #3732, Bv was kept constant at $10-15$ G; other parameters were the same as in #3749. In this magnetic configuration, a distinctive feature was found in the images captured by the high-speed and medium speed cameras. Figure 3 shows H_α images captured by the medium-speed camera. Figure 3(a) shows the vertically extended plasma near the CS at 0.398 s. The slab structure is attributed to plasma production in the fundamental harmonic region by 8.2 GHz ECH. In Figs. 3(b) at 0.406 s and (c) at 0.414 s, the topology of these emission profiles changes and the emission peak shifts to the outer side. Tangential images captured by the medium-speed camera enabled us to obtain the radial position of the plasma in detail. Figures 4 (a) and (b) show the time evolution of Ip and a contour plot of the medium-speed camera image data, which is extracted in the radial direction of the one vertical point indicated by a dotted line in Fig. 3(b), respectively. Figures 4 (c) and (d) corresponds to the expanded time scale of Fig. 4 at $0.5-0.55$ s. As these graph shows, the plasma current changed repeatedly, and the radial position of H_α emission correspondingly shifted at the inner($R < 1.0$ m) and outer($R > 1.0$ m) regions. Interestingly, both cycles were completely the same. When H_α emission had a peak in the inner region, Ip became higher than the H_α emitted in the outer position.

To examine the origin of the plasma behavior, high-speed camera images captured at high time resolution were used. Figure 5 shows the time evolution of Ip from Fig. 4 at an expanded time scale, $0.4-0.416$ s. Figure 6 shows the time evolutions of images at the

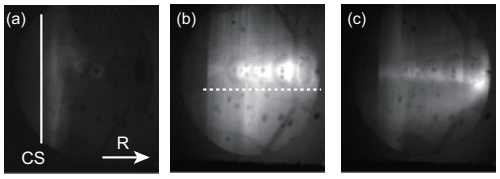

Fig. 3 Medium-speed camera pictures of #3732.

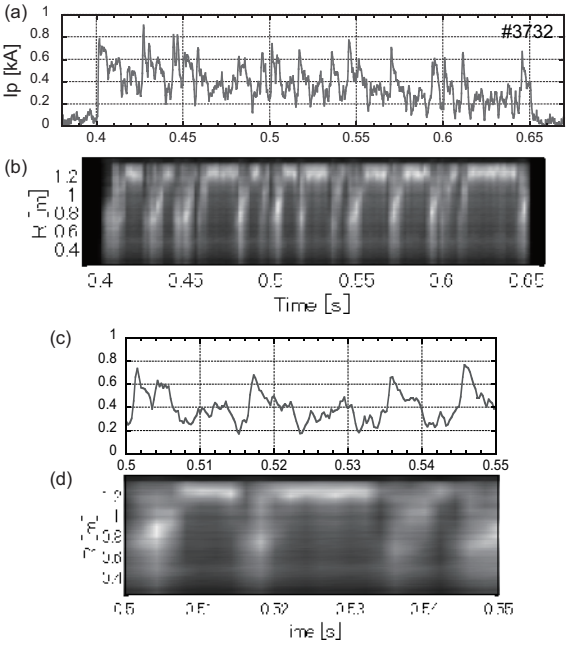

Fig. 4 Time evolution of Ip and contour plot in radial direction of H_α emission captured by medium-speed camera.

beginning of the discharge #3732. Since the high-speed camera has a horizontal view, as shown in Fig. 1, the CS is identified at the center of the images. The capture time of images (a)-(h) run from 0.4002 s to 0.4009 s at 0.0001 s intervals. In Fig. 6(a), vertically expanded structure corresponding to the fundamental harmonic region of 8.2 GHz ECH was observed. In the upper part of Fig. 6(b), a cloud separate from the slab plasma was confirmed. The separated structure gradually moved away from the slab plasma as shown in Figs. 6 (d) to (f). The separated plasma stopped in the radial direction and expanded in size, as shown in Figs. 6 (f) to (h). After this sequence, Ip was considered to increase. Therefore, it was clarified that the plasma separated before the increase in Ip.

Figure 7 shows the radial profiles of the image data captured by the medium-speed camera. The vertical positions of the data are the same as in Fig. 3. The separation of the plasma described previously occurred between 0.4 s and 0.410 s. After the plasma separation, the separated structure showed a peak and held at $R \sim 0.6-0.8$ m, after which Ip increased

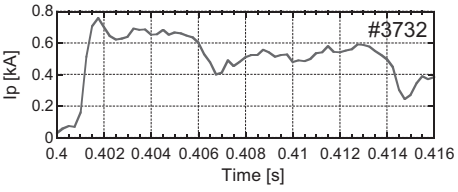

Fig. 5 Time evolution of Ip in expanded time scale.

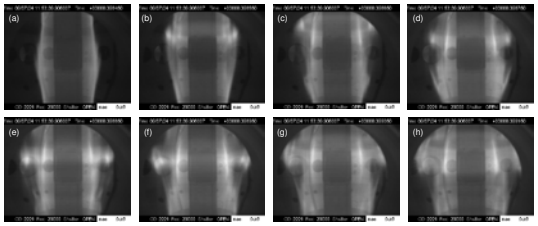

Fig. 6 High-speed camera pictures at #3732.

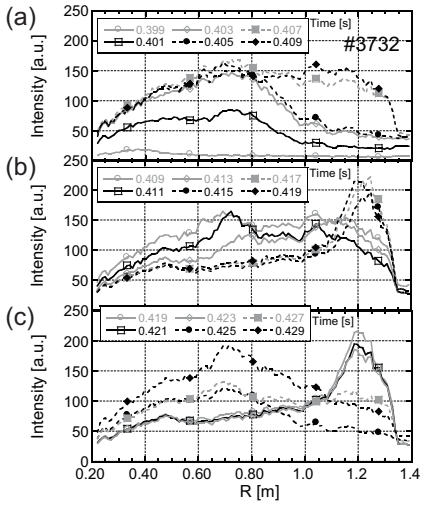

Fig. 7 Radial profile of H_α emission captured by medium speed camera.

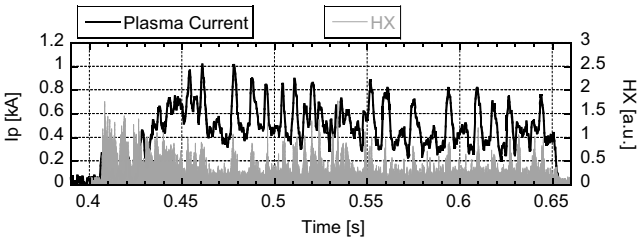

Fig. 8 Time evolution of Ip and hard X-ray spectrum.

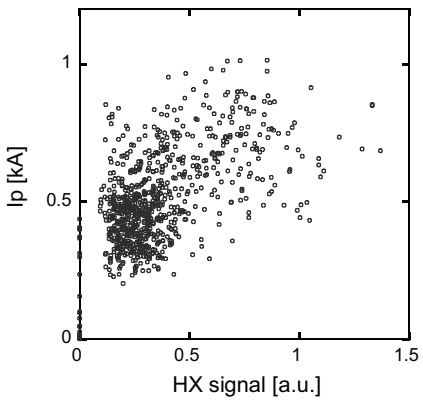

Fig. 9 Ip as a function of hard X-ray spectrum.

rapidly. While the stagnation continued until 0.405 s, Ip remained higher than that after 0.407 s. Therefore, the stagnation of the separated structure, which was maintained at $R \sim 0.6 - 0.8\ m$, is believed to have caused the increase in Ip. The peaked profile of the stagnation plasma became flat at 0.407 s, and Ip simultaneously decreased. The flat profile persisted until 0.413 s. After that, the H_α emission shifted to the outer region and showed a peak near the QUEST chamber at $R \sim 1.2{-}1.3\ m$. Then, Ip correspondingly decreased to a greater degree. The peaked profiles in the outer region terminated at 0.423 s. High-speed camera measurements showed the slab plasma without the separated structure after 0.423 s, and the separation of the plasma occurred again between 0.423 s and 0.425 s. Thus, the sequence in the plasma behavior described above was repeated in this discharge. Although Ip increased with the repetitive change of H_α signal in this experiment, the sheet-shaped plasma did not change into the tokamak equilibrium state when Ip increased. One of the reasons may be RF power. As shown in reference [4], current jump deeply depends on the RF power. In the CPD experiment, threshold power of RF for current jump is $20 \sim 30kW$. According to the CPD results, $160 \sim 240\ kW$ is considered to be needed for current jump in QUEST because the volume of the QUEST chamber is about 8 times larger than that of CPD. We have not achieved the RF power up to $160 \sim 240\ kW$ in QUEST.

Hard X-ray measurements yielded useful information associated with the relationship between Ip and plasma separation. Figure 8 shows the time dependence of Ip and the raw output of the hard X-ray data. In this experiment, the magnetic configuration was the same as that of #3732, but no information about the radial position of the plasma was available because the camera was aligned differently. As shown in this figure, Ip increased when the hard X-ray signal increased and vice versa. Figure 9 shows Ip as a function of hard X-ray signal. The plasma current is positively correlated with the hard X-ray signal. This result suggests that high-energy electrons were generated by the stagnation of the plasma at $R \sim 0.6 - 0.8\ m$. Since the second harmonic resonance heating region of electrons is at $R \sim 0.65\ m$ in this magnetic configuration, electron heating produced the high-energy electrons, which may be concerned with the increase of Ip.

4. Summary

Non-inductive discharge using 8.2 GHz ECH was performed in QUEST. In an open magnetic field structure, Ip depended on Bv when Bv at $R \sim 0.64\ m$ and $Z \sim 0.0\ m$ changed from 0 to 35 G. The n-index (decay index) was constant. Ip had a maximum at $Bv \sim 10 - 15\ G$. When Bv was kept constant at $10{-}15\ G$, it was confirmed that part of the slab plasma near the CS separated and moved radially outward.

Ip was related to the radial position of H_α emission captured by the medium-speed camera. When the separated plasma stopped at $R \sim 0.6 - 0.8\ m$, the Ip correspondingly increased. During plasma stagnation at $R \sim 0.6 - 0.8\ m$, Ip remained high. After the plasma shifted to the region near the vacuum chamber, Ip decreased. Hard X-ray measurements in an experiment with the same external magnetic field configuration, Ip increased when the hard X-ray signal increased and vice versa. This result suggests that high-energy electrons are generated by the effect of the plasma stagnation at $R \sim 0.6 - 0.8\ m$.

Acknowledgments

This work is supported by the NIFS Collaboration Research Program (NIFS05KUTR013). This work is partially supported by a Grant-in-Aid for JSPS Fellows (No. 20-5343).

[1] M. Peng, *et al.*, Phys. Plasmas, **7**, 1681, (2000).
[2] Y. Takase, *et al.*, Nucl. Fusion, **46** S598, (2006).
[3] T. Maekawa, *et al.*, Plasma Sci. Technol. **8** 95 (2006).
[4] T. Yoshinaga, *et al.*, PFR series **8**, 0100, (2009).
[5] Y. Nakashima *et al.*, J. Nucl. Mater., **363-365**, 616 (2007).
[6] N. Nishino *et al.*, Plasma Fusion Res., **1** 035 (2006).
[7] Y. Higashizono *et al.*, J. Plasma Fus. Res., **2** S1087 (2007).
[8] D.P. Stotler *et al.*, J. Nucl. Mater. **313-316**, 1066 (2003).
[9] H. Zushi *et al.*, J. Nucl. Mater. **363-365**, 1429 (2007).